Desalination and Water Treatment
www.deswater.com

doi: 10.5004/dwt.2019.24170

159 (2019) 365–376
August

Adsorption of methyl blue from solution by carboxylic multi-walled carbon nanotubes in batch mode

Mengmeng Yang, Xiaoyu Li, Weili Wang, Shusheng Zhang, Runping Han*

College of Chemistry and Molecular Engineering, Zhengzhou University, No 100 of Kexue Road, Zhengzhou 450001 China, Tel. +86 371 67781757, Fax +86 371 67781556, email: 1582415059@qq.com (M. Yang), 1035768747@qq.com (X. Li), 1063455250@qq.com (W. Wang), zsszz@126.com (S. Zhang), rphan67@zzu.edu.cn (R. Han)

Received 28 October 2018; Accepted 21 March 2019

ABSTRACT

To enhance adsorption property of multi-walled carbon nanotubes (MWCNTs), the surface was modified by oxidation with sodium hypochlorite solution and mCNTs was obtained. Characterization of mCNTs was performed by FTIR, XRD, XPS, RS and TEM and there were more carbonyl group and hydroxyl group on surface of mCNTs. The adsorption property toward cationic dye methylene blue (MB) from solution was presented. The results showed that the adsorption capacity of mCNTs was significantly higher than that MWCNTs. The adsorption capacity from experiment was up to 120.1 mg·g^{-1} at 293 K. Equilibrium data of MB adsorption can be better predicted by Koble-Corrigan model while kinetic data can be predicted by pseudo-first-order kinetic model. Thermodynamics study indicated the exothermic, spontaneous and physicochemical process. MB-loaded mCNTs was secondly used as adsorbent to remove anionic dye, Congo red (CR). It was proved that MB-loaded mCNTs had good adsorption capacity for CR. It was implied that mCNTs can be promising to remove dyes from solution.

Keywords: Carboxylic multi-walled carbon nanotubes; Adsorption; Methylene blue; Regeneration

1. Introduction

With the rapid development of Chinese dye industry, the wastewater produced has become the main source of water pollution. The dye wastewater has deep color, high COD and BOD values, complex and variable composition, so how to effectively remove dyes from solution is a still problem [1]. At present, the most commonly used methods for removing dye wastewater include chemical coagulation, ozone oxidation, ion exchange, Fenton reagent, electrochemical photocatalytic degradation, and adsorption [2–5]. As a result of low cost, high efficiency and simple operation, adsorption method is widely used in actual wastewater treatment [6–8].

In 1991, carbon nanotubes (CNTs) were synthesized by Iijima of the Basic Research Laboratory of NEC Corporation in Japan [9], which had a high specific surface area as a one-dimensional nanomaterial and a rich void structure to make carbon nanotubes more widely application [10]. CNTs mainly include single-walled carbon nanotubes (SWCNTs) and multi-walled carbon nanotubes (MWCNTs). However, since the nanomaterials have a large van der Waals force, the carbon nanotubes had been easily agglomerated together, which greatly limited their application. Therefore, it is necessary to modify the surface of carbon nanotubes to obtain greater dispersion in solvents. A commonly used surface modification method is to introduce an amino group or a carboxyl group on the surface to improve the dispersibility. In the method of introducing a carboxyl group, HNO_3, H_2SO_4, H_2SO_4-H_2O_2 and $KMnO_4$ are mostly used [11–14], but these strong oxidation methods have destroyed the structure of carbon nanotubes. So mild oxidant can be selected like sodium hypochlorite (NaClO). Although there are some reports about the modification of multi-walled carbon nanotubes with sodium hypochlorite [15–17], but there was seldom about dye adsorption on this modified multi-walled carbon nanotubes (mCNTs).

*Corresponding author.

The aim of the present study was to prepare mCNTs nanocomposite with carboxylic group for removal of methylene blue (MB, cationic dye) from solution. The effect of pH and salt concentration on the adsorption quantity were performed and MB-loaded mCNTs was reused after desorption. The mechanism of adsorption was discussed. Furthermore, MB-loaded mCNTs was recycled in second adsorption to remove anionic Congo red (CR) from solution.

2. Experimental section

2.1. Experimental instruments and materials

721 spectrophotometer (Shanghai Third Instrument Co., Ltd.); muffle furnace SX-4-10 (Shanghai Electric Furnace Factory); pH meter (Shanghai Third Analytical Instrument Factory); SHZ-82 constant temperature water bath oscillator Jiangsu Taicang Medical Machinery Factory); epichlorohydrin (ECH, Tianjin Kemiou, China); Multi-walled carbon nanotubes (MWCNTs, ID: 3–5 nm, OD: 8–15 nm, length: 50 μm, Macklin, China); sodium hypochlorite solution (NaClO, Macklin, China); Congo red; hydrochloric acid; hydrogen sodium oxide, etc. (all of which are of analytical grade).

2.2. Preparation of carboxylic multi-walled carbon nanotubes

Purification: Multi-walled carbon nanotubes (MWCNTs) were calcined in a muffle furnace at 460°C for 30 min to remove amorphous carbon.

Preparation: 0.5 g of purified MWCNTs and 300 mL of 30% NaClO solution were added to a 500 mL conical flask. Then kept the mixture at room temperature for 12 h with continuous and centrifuge to adjust pH = 7, and dried the product at 60°C in the vacuum drying oven. Carboxylic multi-walled carbon nanotubes (mCNTs) were obtained after 12 h.

2.3. Characterization of MWCNTs and mCNTs

The characterizations were performed by several analytical techniques, such as TEM (TECNAIG2F20-S-TWIN, American), FTIR (Nicolet iS50, American) and Raman spectroscopy (Raman, LabRAM HR Evolution, France). X-ray diffraction (XRD) analysis was performed by a PAN alytical X'Pert PRO instrument (The Netherlands). The binding energy of mCNTs before and after MB adsorption was analyzed by X-ray photoelectron spectroscopy (XPS, ESCALAB 250Xi, England). The pH of zero point charge (pHzpc) about mCNTs and MWCNTs was measured.

2.4. MB adsorption onto mCNTs in batch mode

The test was carried out in batch mode. 10 ml MB solution and a certain amount of mCNTs or MWCNTs were added into a 50 mL conical flask, shaking the mixture in a shaker for a certain time, then taking it up, centrifuging and diluting it to determine the residual concentration of methylene blue. Finally calculated the adsorption capacity and removal efficiency of carbon nanotubes to MB (MB was analyzed by visible spectrophotometry, maximum absorption wavelength 665 nm).

$$q_e = \frac{V(C_0 - C_e)}{m} \tag{1}$$

$$p = \frac{(C_0 - C_e)}{C_0} \times 100\% \tag{2}$$

where q_e - unit adsorption amount ($mg \cdot g^{-1}$), C_0 - concentration of solution before adsorption ($mg \cdot L^{-1}$), C_e - concentration of solution after adsorption equilibrium ($mg \cdot L^{-1}$), V - volume of solution (L), m - adsorbent weight (g).

2.5. Desorption study

The best method (75% ethanol) was used for multiple desorption and regeneration. MB-loaded mCNTs was obtained for MB adsorption at initial concentration 150 $mg \cdot L^{-1}$ (pH = 7.5) at 303 K and the first-time adsorption quantity q_e was calculated. Then, MB-loaded mCNTs was washed with distilled water to remove unabsorbed MB and was dried at 60°C. Next step the desorption would be done. MB-loaded mCNTs (solid solution volume, 0.8 g/L) and 75% ethanol were mixed into a conical flask, and oscillated with 303 K to obtain equilibrium, then the concentration of supernatant was measured. The adsorbent after desorption was cleaned and dried, and then re-adsorbed under the same experimental conditions as the first adsorption. The unit adsorption amount of the regenerated adsorbent was calculated as q_r. The desorption efficiency d and regeneration efficiency r were calculated into Eqs. (3) and (4). Multiple desorption and regeneration were the same as the above primary desorption and regeneration.

$$d = \frac{m_d}{m_0} \times 100\% \tag{3}$$

$$r = \frac{q_r}{q_m} \times 100\% \tag{4}$$

where m_d was the mass (mg) of the adsorbed substance desorbed in the desorption process, and m_0 was the mass (mg) of the adsorbate on the adsorbent before desorption.

2.6. Congo red adsorption onto surface of MB-loaded mCNTs in batch mode

A certain amount absorbent of MB-loaded mCNTs (solid solution volume, 0.8 g/L) and 10 ml C_0 = 500 $mg \cdot L^{-1}$ CR (pH = 6.5, T = 303 K) were added to a 50 mL conical flask, shaking the mixture in a shaker for a certain time, then taking it up, centrifuging and diluting it to determine the residual concentration of CR. CR was analyzed by visible spectrophotometry at the maximum wavelength (499 nm). The calculation of unit adsorption amount was the same as MB adsorption on mCNTs.

3. Results and discussion

3.1. Characterization of adsorbents

3.1.1. pHzpc of mCNTs and MWCNTs

pHzpc can predict the charge on the surface of the adsorbent at a certain pH value, so it is necessary to dis-

cuss the effect of solution pH on adsorption quantity. The results for measurement of pHzpc are shown in Fig. 1. It was seen that the pHzpc of MWCNTs was 7.0, while mCNTs became 6.8. The pHzpc of mCNTs moved toward the acidic direction, which indicated that the acidic group had been successfully introduced into the surface of multi-wall carbon nanotubes.

3.1.2. Infrared spectrum

FTIR can offer information of some functional group before and after modification. The FTIR of MWCNs and mCNTs are shown in Fig. 2. It was observed from the mCNTs that a strong absorption peak appeared at 1712 cm^{-1}, which indicated the presence of C=O on the surface of mCNTs. The absorption peak in the range of 3600–3300 cm^{-1} (ranging from 3440 cm^{-1} to 3439 cm^{-1} after oxidation) indicated the presence of carbon nanotube surface hydroxyl. And MWCNTs basically had no obvious absorption peak, which was similar to Zhao [18]. Thus, it could be seen that the surface of multi-walled carbon nanotubes modified by sodium hypochlorite was oxidized so that the surface of mCNTs had carboxyl and hydroxyl groups. The FTIR of MB-loaded mCNTs had two major changes. One was the addition of two peaks at 1118 cm^{-1} and 1034 cm^{-1}, where the peaks were the stretching vibration of C-S on MB. The absorption peak at 1596 cm^{-1} was strengthened, which was due to the skeleton vibration of benzene ring, indicating that MB had been successfully loaded onto mCNTs.

3.1.3. Transmission electron microscope

In order to study the surface morphology of carbon nanotubes, it is necessary to do the experiment of TEM. The TEM images of MWCNTs and mCNTs are illustrated in Fig. 3. It was seen that the average external diameter of the two kinds of carbon nanotubes was about 30 nm, whose internal diameter was about 10 nm and the medium hollow tubular structure obviously. The MWCNTs (Fig. 3a) was thicker, and the end of the tube was mostly closed. There were black particles in the tube as impurity such as catalyst particles and amorphous carbon on the original carbon nanotube. The mCNTs (Fig. 3b) had few impurities and there was obvious fracture trace at the end of the pipe body. This was due to the sodium hypochlorite oxidation treatment not only to remove the impurities in the carbon nanotubes, but also to make the defect part of the carbon nanotubes (such as bending and end cap) eroded and disconnected, which was similar to other experimental result [16].

3.1.4 Scanning electron microscope

In order to explore the surface characteristic changes of carbon nanotubes before and after modification, the adsorbent is analyzed by SEM (Fig. 4). The tubular structures of MWCNTs were wound together, some of which were in the form of aggregates, with a length of 50 microns, an inner diameter of 3–5 nm and an outer diameter of 8–15 nm. Compared with MWCNTs, mCNTs had lower degree of entanglement, shorter length and basically unchanged inner and outer diameter. The lower degree of aggregation

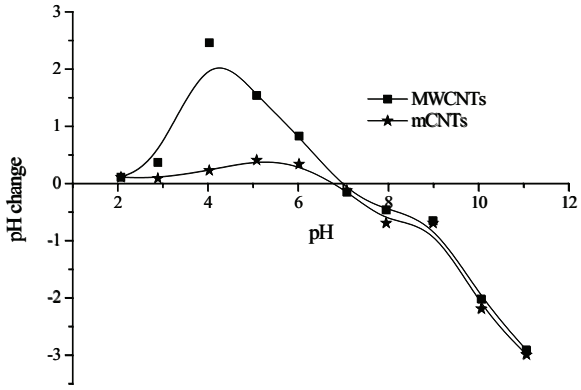

Fig. 1. The isoelectric point of mCNTs and MWCNTs (T = 303 K, C_{NaCl} = 0.01 mol·L^{-1}).

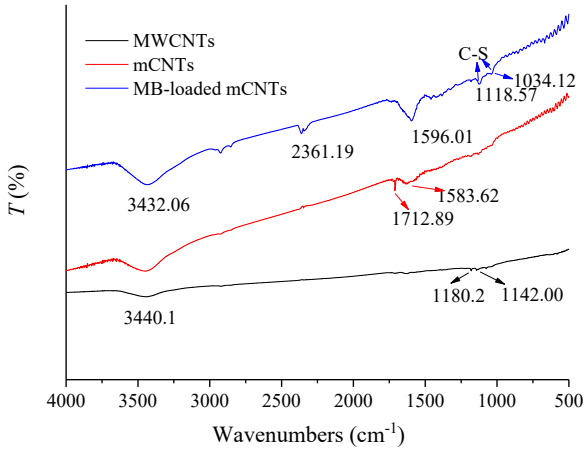

Fig. 2. FTIR spectra of MWCNTs, mCNTs and MB-loaded mCNTs.

in mCNTs was not only related to the carboxyl group, but also to the shortening of the nanotube lengths.

3.1.5. Raman analysis

The Raman spectra (RS) could also offer some useful information and RS of MWCNTs and mCNTs are shown in Fig. 5. Two peaks of 1350 cm^{-1} and 1580 cm^{-1} are seen from Fig. 5. Peak at 1350 cm^{-1} was so-called D-band, which was related to the carbon atoms of the disordered SP^3 hybridized carbon nanotubes. Another peak at 1580 cm^{-1} was so-called G-band that was related to the symmetry of the interlayer mode of graphite E_2G.

The ID/IG value of MWCNTs was 0.99, which became 1.02 after modification. This indicated that the surface properties of MWCNTs were greatly improved after 30% sodium hypochlorite solution purification [19].

3.1.6. XPS analysis

In order to further determine the carboxyl and the introduction of MB on mCNTs, the surface elements of

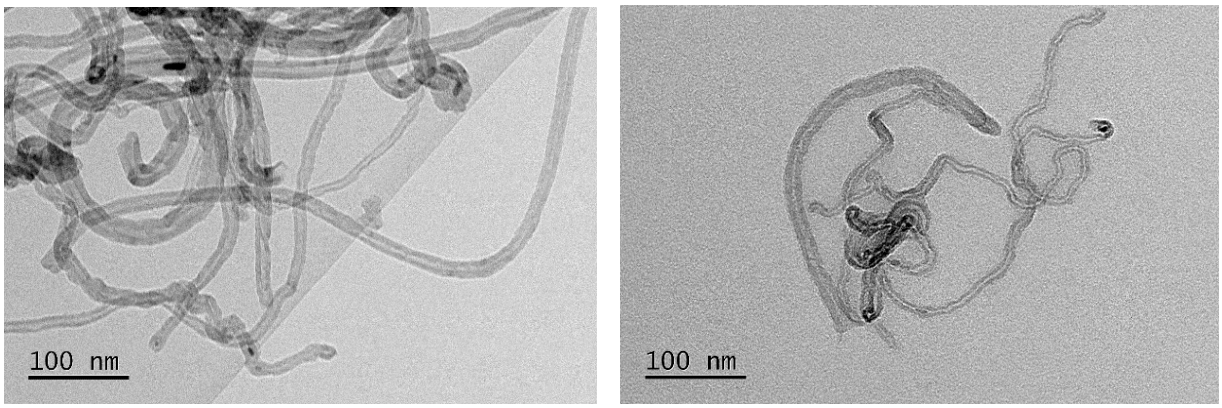

Fig. 3. Transmission electron microscopy (TEM) images of MWCNTs (left) and mCNTs (right).

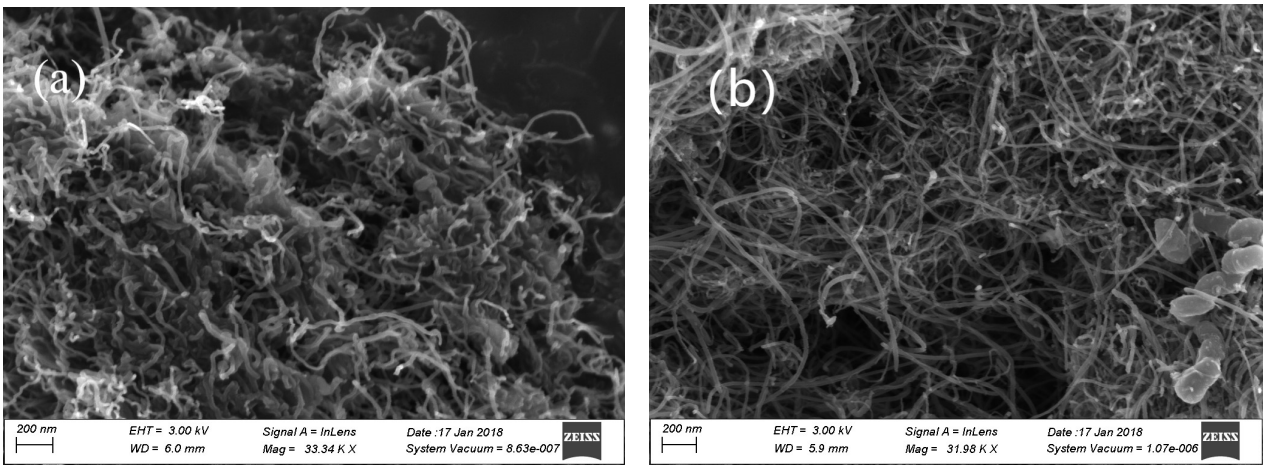

Fig. 4. Scanning electron microscopy (SEM) images of MWCNTs (a) and mCNTs (b).

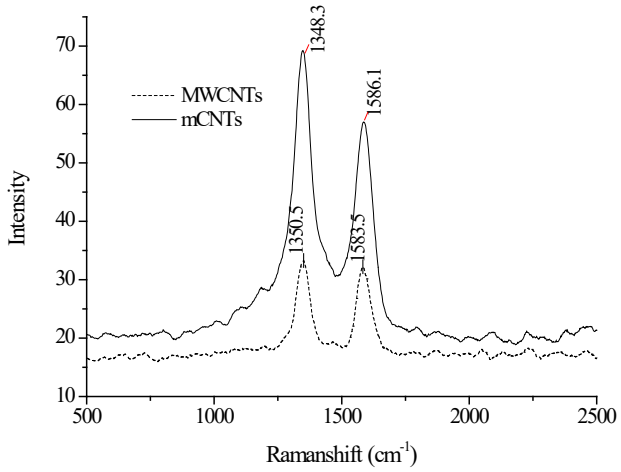

Fig. 5. Raman spectra of MWCNTs and mCNTs.

mCNTs and MB-loaded mCNTs were analyzed by XPS, and the results are shown in Fig. 6. It is known from Fig. 6a that there were C and O elements in mCNTs while there were N and S element from Fig. 6b after MB adsorption, which S and N were from MB (S2p peak at 168 eV, N1s peak at 345 eV), indicating that methylene blue has been successfully adsorbed onto surface of mCNTs. Fig. 7 shows the peaks of O1s before and after MB adsorption. From O1s peak, the molar ratio of O/C before and after adsorption of MB was 59.6% and 51.9%, respectively, indicating that the oxygen content decreased after adsorption of MB, which may be the combination of carboxyl oxygen and MB on mCNTs. The peaks of –OH and H_2O increased from 533.78 eV and 536.40 eV to 533.87eV and 537.35 eV after MB adsorption. These differences indicated that there was electrostatic attraction between the carboxyl or hydroxyl groups on the adsorbed surface and the positive groups on the dye molecules.

3.1.7. BET analysis

The specific surface area of adsorbents was specified by the BET method. The BET surface areas of carbon nanotubes before and after modification were 159.3, 79.81 m^2/g, respectively. This may be due to the formation of functional groups on the surface of carbon nanotubes oxidized by sodium hypochlorite. After one cycle (first adsorption saturation, then desorption), the BET surface area of mCNTs

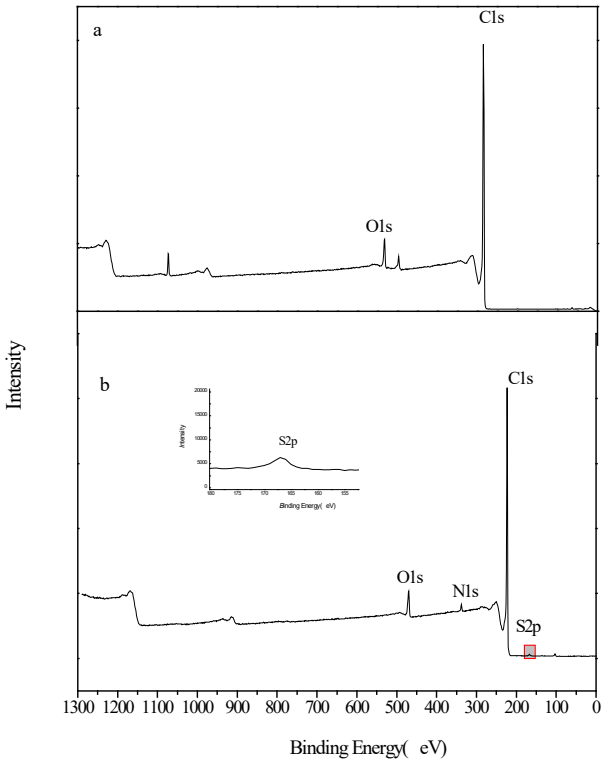

Fig. 6. The survey XPS spectra of mCNTs (a) and MB-loaded mCNTs (b).

was 95.51 m^2/g, which indicated that 75% ethanol had successfully desorbed part of methylene blue adsorbed on carboxyl carbon nanotubes, making the specific surface area of mCNTs larger.

3.1.8. XRD analysis

X-ray diffraction is an effective method to study the structure of carbon materials. The XRD patterns of MWCNTs and mCNTs are displayed in Fig. 8. There were two diffraction peak appears in the same position, namely the two characteristic peaks of carbon nanotubes (002) diffraction peak (2θ = 26°) and (100) (2θ = 43°), respectively [20]. The position of the two peaks did not change, indicating that carboxylation did not destroy the crystalline structure of carbon nanotubes. However, after one cycle of mCNTs the intensity of (002) peaks became stronger than the mCNTs, indicating a higher degree of crystallinity. The two peak positions did not change basically, indicating that the mCNTs material prepared was still stable.

3.2. Adsorption of methylene blue

3.2.1. Effect of adsorbent dose on the adsorption of methylene blue by mCNTs

In order to study the effect of mCNTs dosage on the adsorption of MB, the mCNTs with different mass were taken and put into conical flask respectively. The results are shown in Fig. 9. It was known that values of q_e decreased

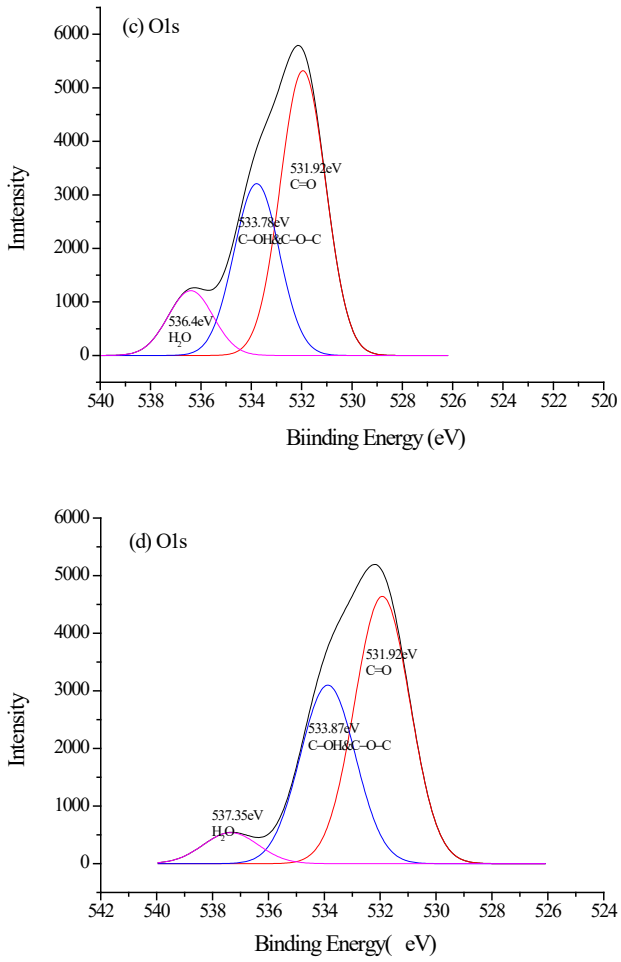

Fig. 7. High-resolution oxygen 1s XPS spectra of mCNTs (c) and MB-loaded mCNTs (d).

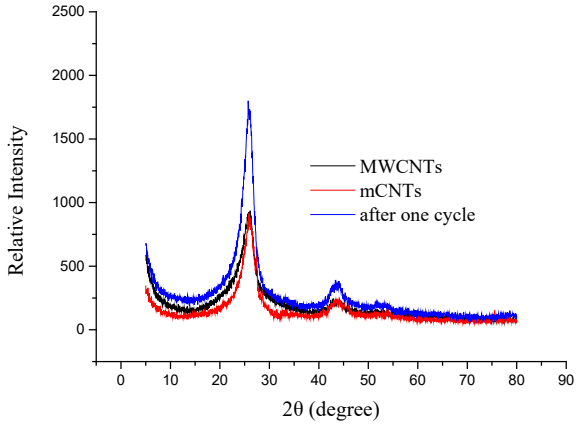

Fig. 8. XRD patterns of MWCNTs and mCNTs.

with the increase of adsorbent dose (solid-liquid ratio), while the removal efficiency gradually increased. The reason was that as the solid-liquid ratio increased, the number of active sites was more with higher adsorbent dose, so the removal efficiency increased; However, the surface sites of

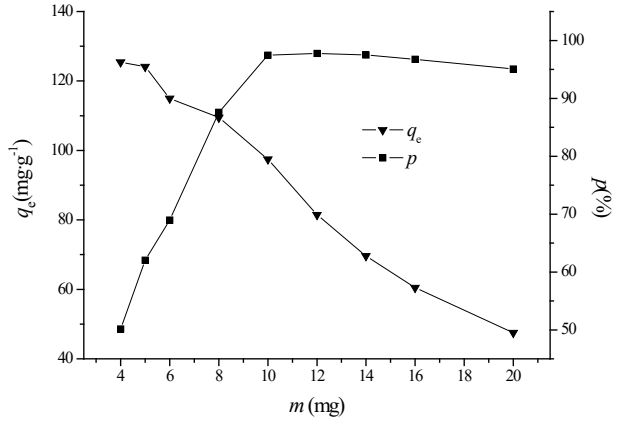

Fig. 9. Effect of adsorbent dose on MB adsorption (T = 303 K, C_0 = 100 mg·L^{-1}).

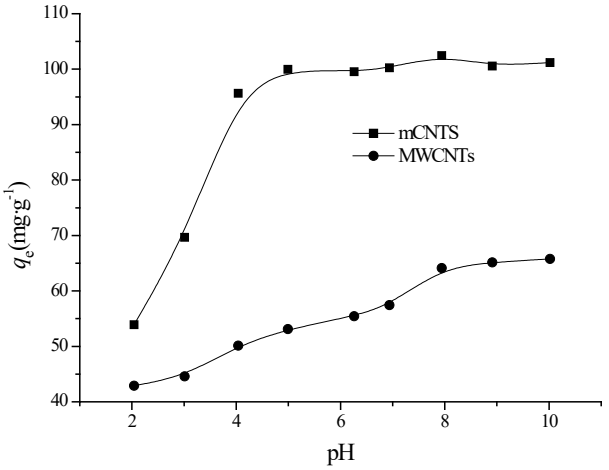

Fig. 10. Effect of solution pH on MB adsorption (T = 303 K, C_0 = 100 mg·L^{-1}).

adsorbents may not be saturated or the adsorption mass assigned to each adsorbent becomes less, resulting in a decrease in the unit adsorption amount [21,22]. The concentration of mCNTs in subsequent experiments was 0.8 g·L^{-1}.

3.2.2. Effect of pH on adsorption

The pH value of the solution is an important factor affecting the adsorption effect. The existence form of the adsorbate and the surface charge of adsorbent are all affected by solution pH. The effect of solution pH on values of q_e is shown in Fig. 10.

It was observed that the adsorption capacity of MB was dependent of solution pH and the trend was similar about mCNTs and MWCNTs. There was smallest of adsorption quantity at pH = 2. At lower pH, the positively charged surface of the mCNTs would be electrostatic repelled with the cationic dye MB, and H^+ in solution would also compete with MB for adsorption sites. Conversely, as solution pH increased, the positive charge on the surface of the adsorbent decreased, the surface functional group –COOH became –COO^-, which was susceptible to MB adsorption [23]. In conclusion, values of q_e about MB on mCNTs or MWCNTs became larger, and the former was higher. This showed that there was higher adsorption capacity of mCNTs. Comprehensive analysis, the subsequent experiments were not adjusting solution pH (near pH 7.5).

3.2.3. Effect of salt ion on adsorption of MB

In practice, salt ions are often contained in wastewater, so it is necessary to discuss the effect of salinity on adsorption. The result is presented in Fig. 11.

For mCNTs, the presence of coexisting ions in the solution was not conducive to the adsorption, which indicated that the main force between the adsorbent and the adsorbent was electrostatic attraction. It is also seen from Fig. 11 that the effect of Ca^{2+} on adsorption is more detrimental than that of Na^+. Because Na^+ and Ca^{2+} in the solution could compete with the positively charged MB molecules on the surface, value of q_e decreased with the increase of salt ions concentration. At the same time, the charge of Ca^{2+}

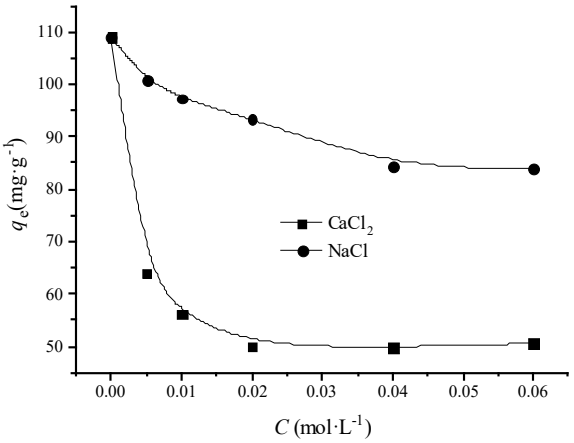

Fig. 11. Effect of NaCl and $CaCl_2$ concentration on MB adsorption (T = 303 K, C_0 = 100 mg·L^{-1}).

was greater than Na^+, and the contribution to ionic strength was also larger from $CaCl_2$ at same concentration. The volume of Ca^{2+} was larger than that of Na^+, and the larger Ca^{2+} blocked some adsorption sites on mCNTs when adsorbing MB, so $CaCl_2$ coexistence had a greater negative effect on MB adsorption. So there are electrostatic attraction between mCNTs and MB.

It was also observed that there was still some adsorption capacity at higher salt concentration (48 mg·g^{-1} for $CaCl_2$ and 86 mg·g^{-1} for NaCl). This result implied that other actions, which were not affected by ionic strength (such as hydrogen bond and Van der Waals' force), were existed during adsorption process. Similar result was observed about LG adsorption onto PEI-modified CNTS [24]. So mCNTs can be efficiently to remove toxic dyes from wastewater.

3.2.4. The effect of contact time on adsorption

The initial concentration of MB in the solution was C_0 = 100 mg·L^{-1}, and the effect of kinetic time on adsorp-

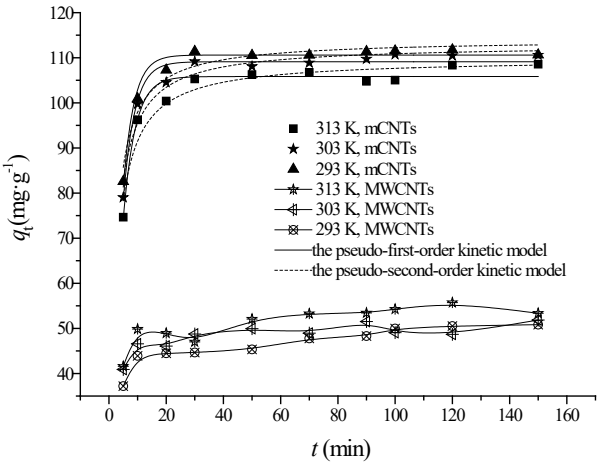

Fig. 12. Effect of contact time on MB adsorption (C_0 = 100 mg·L^{-1}).

tion quantity at various temperatures is shown in Fig. 12. According to Fig. 12, the adsorption of MB on mCNTs was basically balanced in 30 min, which meant the time of adsorption was very short, and the adsorption of MB on mCNTs was significantly higher than that of the MWCNTs. This result also showed that the modification was valuable. As the temperature increased, the adsorption amount decreased, indicating that the adsorption process of MB on mCNTs was exothermic, which was consistent with the results of other studies on MB adsorption of mCNTs [25].

Kinetic models can be used to predict the kinetic process. Two models, pseudo-first-order kinetic model and pseudo-second-order kinetic model, are selected.

The expression of pseudo-first-order kinetic model [26]:

$$q_t = q_e(1 - e^{-k_1 t}) \tag{5}$$

The expression of pseudo-second-order model [27]:

$$q_t = \frac{k_2 q_e^2 t}{1 + k_2 q_e t} \tag{6}$$

where q_t (mg·g^{-1}) is the adsorption capacity at time (t) and q_e (mg·g^{-1}) is the adsorption capacity at equilibrium; k_1 (min^{-1}) and k_2 (g·mg^{-1}·min^{-1}) are the rate constant.

The kinetic data were fitted by nonlinear regressive analysis and the parameters of kinetic models, determined coefficients (R^2) and errors (*SSE*) are listed in Table 1. The fitted curves are also illustrated in Fig. 12.

It is seen from Table 1 that the kinetic process of MB adsorption onto mCNTs was better fitted by the pseudo-first-order kinetic model ($R^2 > 0.95$). In the meantime, the *SSE* was relatively smaller. The difference between values of q_e with experiments was smaller at same condition. This showed that pseudo-first-order kinetic model can be used to describe the kinetic process and predicted the adsorption quantity, while the adsorption process was mainly physical adsorption. At the same time, the pseudo-second-order kinetic model was also to fit the experimental results according the fitted results, indicating that the adsorption process had chemical adsorption. Therefore, the adsorption of MB on mCNTs had both physical and chemical adsorption.

Table 1
Parameters of kinetic models for MB adsorption

Pseudo-first-order equation					
T/K	$q_{m(exp)}$ (mg·g^{-1})	$q_{m(theo)}$ (mg·g^{-1})	$k_1 \times 10^{-2}$ (min^{-1})	R^2	*SSE*
293	110.6	110.6±0.5	26.6±0.9	0.975	16.5
303	110.6	109.1±0.6	25.2±1.1	0.969	24.0
313	108.6	105.8±0.8	24.1±1.3	0.955	38.1
Pseudo-second-order equation					
T/K	$q_{m(exp)}$ (mg·g^{-1})	$q_{m(theo)}$ (mg·g^{-1})	$k_2 \times 10^{-4}$ (g·mg^{-1}·min^{-1})	R^2	*SSE*
293	110.6	114.1±1.0	53.0±5.9	0.940	40.7
303	110.6	112.9±1.1	48.3±5.4	0.941	45.0
313	108. 6	109.8±1.2	45.5±5.7	0.931	57.1

Note: $SSE = \sum (q - q_c)^2$, q and q_c are the experimental value and calculated value according the model, respectively.

3.2.5. The effect of dye concentration and temperature on adsorption

Dye concentration can affect adsorption quantity. Fig. 13 presents the effect of MB concentration on adsorption quantity at various temperatures.

It is seen from Fig. 13 that the adsorption quantity gradually decreased with the increase of temperature. This meant that the process was exothermic; when the temperature was constant, values of q_e can be increased rapidly with the increase of the equilibrium concentration. Then it gradually stabilized until the adsorption was saturated. At 293 K, values of q_e were up to 121.0, 115.1, 112.0 mg·g^{-1} at 293, 303, 313 K, respectively.

In order to further study the thermodynamic behavior of the adsorption process, four isotherm models of nonlinear expression were selected.

(1) Langmuir model

In 1916, Langmuir first proposed a monolayer adsorption model [28,29]. The formula is:

$$q_e = \frac{q_m K_L C_e}{1 + K_L C_e} \tag{7}$$

where q_m (mg·g^{-1}) is the adsorption amount when the surface of the adsorbent is covered with a monolayer, that is, the saturated adsorption amount; K_L (L·mg·g^{-1}) is the adsorption coefficient, which is related to temperature and heat of adsorption.

It can be seen from Eq. (7) that when the adsorption amount is small, that is, $K_L \cdot C_e << 1$, $q_e = q_m C_e K_L$, which mean q_e is proportional to C_e, and the isotherm is approximately in a straight line.

When the amount of adsorption is large, that is, when $K_L \cdot C_e >> 1$, $q_e = q_m$, which mean the equilibrium adsorption

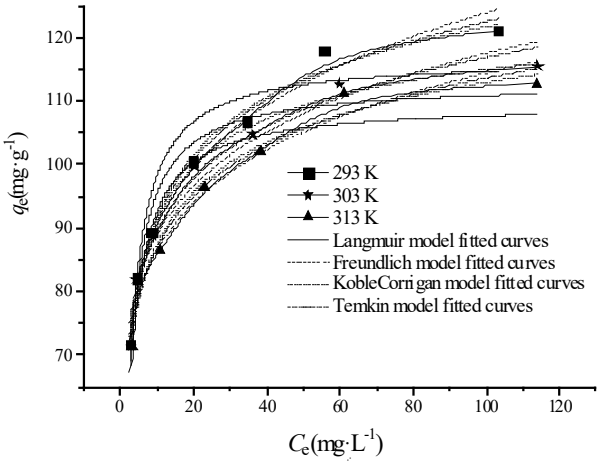

Fig. 13. Adsorption isotherms and fitted curves of MB adsorption onto mCNTs.

amount is close to a fixed value, and the isotherm tend to be horizontal.

(2) Freundlich model

The Freundlich adsorption equation [29] was a nonlinear mode, which was derived by Freundlich in 1907. This is an empirical formula whose equation is as follows:

$$q_e = K_F C_e^{1/n} \tag{8}$$

where K_F and n are Freundlich constants. For the fitted parameter n value, $0.1 < 1/n < 0.5$ is generally considered to be preferential adsorption, which mean it is easy to adsorb; and $1/n > 2$ is difficult to adsorb. Using the two constants K_F and $1/n$, the properties of different adsorbents could be compared.

(3) Temkin model

The Temkin adsorption isotherm form is [29]:

$$q_e = A + B\ln C_e \tag{9}$$

where A and B are the two constants of the equation, respectively.

The above three adsorption equations have a very simple form, and could be transformed into a straight-line equation for drawing fitting, so it is convenient to use. However, according to the energy-related assumptions in the adsorption model, the three adsorption equations reflect different energy relationships in the adsorption process. The energy relationship represented by the Langmuir equation is that the heat of adsorption did not change with adsorption, and the energy of each adsorption point is constant, which is obviously an ideal adsorption. The energy relationship described by the Temkin equation is that the heat of adsorption decreased linearly with the amount of adsorption. The energy relationship represented by the equation of Freundlich is that the heat of adsorption decreased logarithmically with the amount of adsorption. Therefore, the Temkin equation and the Freundlich equation are suitable for uneven surface adsorption.

(4) Koble-Corrigan model

The general form is [29]:

$$q_e = \frac{AC_e^n}{1 + BC_e^n} \tag{10}$$

It is a combination of the Langmuir and Freundlich models. Where A, B and n are parameters of model.

The fitted results according to nonlinear regressive analysis are listed in Table 2 and the fitted curves are also presented in Fig. 13.

It was found from the Table 2 that there were lowest value of R^2 and highest values of SSE from Langmuir model. This indicated that Langmuir model was not used to describe the equilibrium process and the adsorption process was not single-molecule adsorption.

There were highest values of R^2 with lowest values of SSE about Koble-Corrigan model according to Table 2. Furthermore, the fitted curves were very close to experimental points. These showed that Koble-Corrigan model was best to fit the experimental data and could describe the equilibrium process. For Freundlich model and Temkin model, there were also higher values of R^2 and lower values of SSE, which meant that both models also can predict the adsorption process. Parameter $1/n$ from Freundlich model was within 0.1–0.5, which showed that the process easily occurred. Therefore, the adsorption process of MB on mCNTs was uneven multi-molecular layer adsorption.

3.2.6. Thermodynamic parameters of adsorption

(1) The thermodynamic parameters of the adsorption process could be used to infer the adsorption mechanism and understand the adsorption process more clearly at the micro level. The change Gibbs free energy ΔG (J·mol^{-1}), enthalpy change ΔH (J·mol^{-1}) and entropy change ΔS (J·mol^{-1}·K^{-1}) values in the adsorption process were calculated. Value of ΔG can be calculated by Eq. (12).

$$\Delta G = -RT \ln K_c \tag{11}$$

$$\Delta G = \Delta H - T\Delta S \tag{12}$$

where R (8.314 J·mol^{-1}·K^{-1}) is the universal gas constant, T (K) is an adsorption reaction temperature, and K_c is an apparent adsorption equilibrium constant. By using concentration instead of activity, K_c can be calculated by Eq. (13) [30–32]:

$$K_c = C_{ad}/C_e \tag{13}$$

where C_{ad} is the concentration of MB on mCNTs at equilibrium, and C_e is the concentration of MB in solution at the first concentration in isotherm at adsorption equilibrium.

Table 2
Parameters of adsorption isotherm models for MB adsorption

Langmuir					
T/K	q_m (theo)/(mg·g^{-1})		K_L (L·mg^{-1})	*SSE*	R^2
293	116.8±3.6		0.529±0.100	174.7	0.896
303	112.6±2.5		0.550±0.078	77.06	0.941
313	109.6±3.2		0.543±0.110	140.7	0.884
Freundlich					
T/K	K_F		1/*n*	*SSE*	R^2
293	66.2±2.0		0.136±0.009	39.6	0.977
303	67.4±2.5		0.120±0.011	64.9	0.950
313	65.2±2.3		0.122±0.010	45.6	0.962
Temkin					
T/K	A		B	*SSE*	R^2
293	60.8±1.9		13.4±0.6	21.5	0.987
303	62.6±2.3		11.8±0.7	36.5	0.972
313	60.4±2.5		11.5±0.8	32.6	0.973
Koble-Corrigan					
T/K	A	B	n	*SSE*	R^2
293	93.8±6.2	0.555±0.140	0.333±0.100	20.0	0.985
303	98.5±7.0	0.740±0.055	0.466±0.100	14.8	0.986
313	96.5±8.8	0.632±0.210	0.327±0.150	30.0	0.969

(2) Apparent activation energy E_a

The value of E_a reflects the difficulty of the adsorption reaction. Generally, the lower the activation energy, the easier the adsorption reaction occurs, and the faster the adsorption reaction rate is at a certain temperature. The apparent activation energy can be obtained from Arrhenius' formula [32].

$$\ln k = -\frac{E_a}{RT} + \ln A \tag{14}$$

where k is the adsorption rate constant obtained from the model most consistent with the adsorption kinetic curve, E_a (J·mol^{-1}) is the apparent activation energy of the adsorption process; R and T are the ideal gas constant and the adsorption reaction temperature, respectively. A is the pre-factor.

Relative parameters are calculated and the results are listed in Table 3. It was implied from the Table 3 that there be a spontaneous, endothermic, and entropic donor adsorption process ($\Delta G < 0$, $\Delta H < 0$, $\Delta S > 0$). Value of ΔG was negative and the absolute was within 0–20 kJ·mol^{-1}, which meant its physical process; the absolute value of ΔH was also within 0–20 kJ·mol^{-1}, which also indicated its physical process. The positive ΔS^0 value illustrated the increased randomness at the solid-solution interface during adsorption of MB on mCNTs [33]. The value of E_a was 21.9 kJ·mol^{-1} (less than 40 kJ·mol^{-1}) and there was physical action during adsorption process.

3.2.7. Desorption and regeneration

Recycle of adsorbent and recovery of adsorbate will make the treatment process economical and it is essential to recover the adsorbent after adsorption [34–36]. In order to make full use of the mCNTs, the reproducibility of mCNTs was performed. 75% ethanol solution was selected to regenerate the MB-loaded mCNTs. Five times of desorption and regeneration were operated and the results are shown in Fig. 14. As the number of cycles increased, the desorption efficiency became lower and lower, which may be due to the strong combination of MB on mCNTs. The regeneration rate remained high after five times of desorption, which may be that mCNTs did not reach adsorption saturation, so there were still empty adsorption sites on mCNTs.

Table 3
Thermodynamic parameters of MB adsorption onto mCNTs

E_a (kJ·mol^{-1})	ΔH^0 (kJ·mol^{-1})	ΔS^0 (J·mol^{-1}·K^{-1})	ΔG^0 (KJ·mol^{-1})		
			293 K	303 K	313 K
21.9	–8.88	5.00	–7.41	–7.38	–7.31

3.2.8. The second adsorption of Congo red on MB-loaded mCNTs

The secondary adsorption of adsorbent can be used to determine the quality of adsorbent and found whether it can be used for further use. So, it is necessary to study the second adsorption and the effect of salt on adsorption [37,38]. The results in second adsorption were shown in Table 4. It was clearly seen that there was good adsorption quantity toward CR about MB-loaded-mCNTs, which was much higher than mCNTs. Value of q_e about mCNTs for CR was 23.93 mg·L^{-1}, while value of q_e about MB-loaded

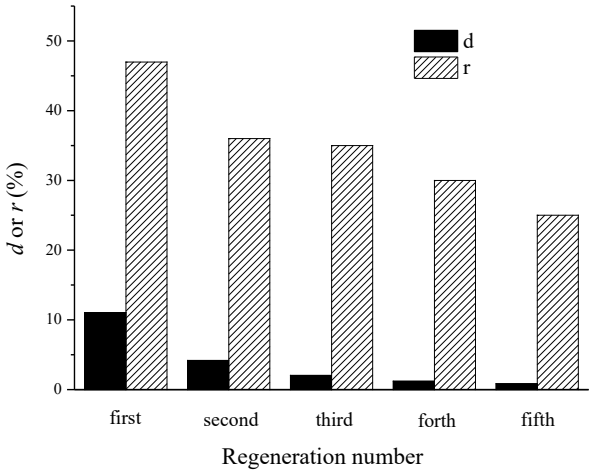

Fig. 14. The desorption/regeneration performance of prepared mCNTs.

Table 4
Second adsorption of CR (C_0 = 500 mg·L^{-1}) on MB-loaded mCNTs (solid solution volume, 0.8 g·L^{-1}).

Adsorbent	No salt	C_{NaCl} = 0.1 mol·L^{-1}
	q_e (mg·g^{-1})	q_e (mg·g^{-1})
mCNTs	23.93	73.39
MB-loaded mCNTs	289.5	162.4

mCNTs was 289.5 mg·L^{-1}, and the adsorption capacity of the latter was 10 times as much as that of the former. This showed that the mCNTs produced had good reusability and was friendly to environment.

The surface of mCNTs is negatively charged and repels anions and the amounts of anionic species adsorbed by mCNTs are often low, so it appears that CR adsorption is enhanced by the surface structure alterations after MB adsorption. The surface property of MB-loaded mCNTs must be significantly different from that of mCNTs. MB bound on mCNTs can act with CR through Van der Waals' forces and hydrogen bonding. This result is similar to found in other studies using biomaterials modified by cationic surfactants to enhance anionic adsorption [39,40] and second adsorption using positive dye-loaded materials as adsorbent to bind anionic dye [41,42].

It was also observed that there was positive to CR adsorption onto mCNTs with coexisted salt because CR was anionic, and the addition of salt reduced the double electrode layer to make CR more accessible to the adsorption surface. If there was electrostatic attraction between anionic CR and MB-loaded mCNTs, the addition of salt may compete with CR and this lead to reduce adsorption quantity. But from the results, electrostatic attraction between MB-loaded mCNTs and CR was not major role.

3.2.8. Mechanism of MB adsorption

The mCNTs had a large number of hydroxyl groups and carboxyl groups, which can interact with dye molecules.

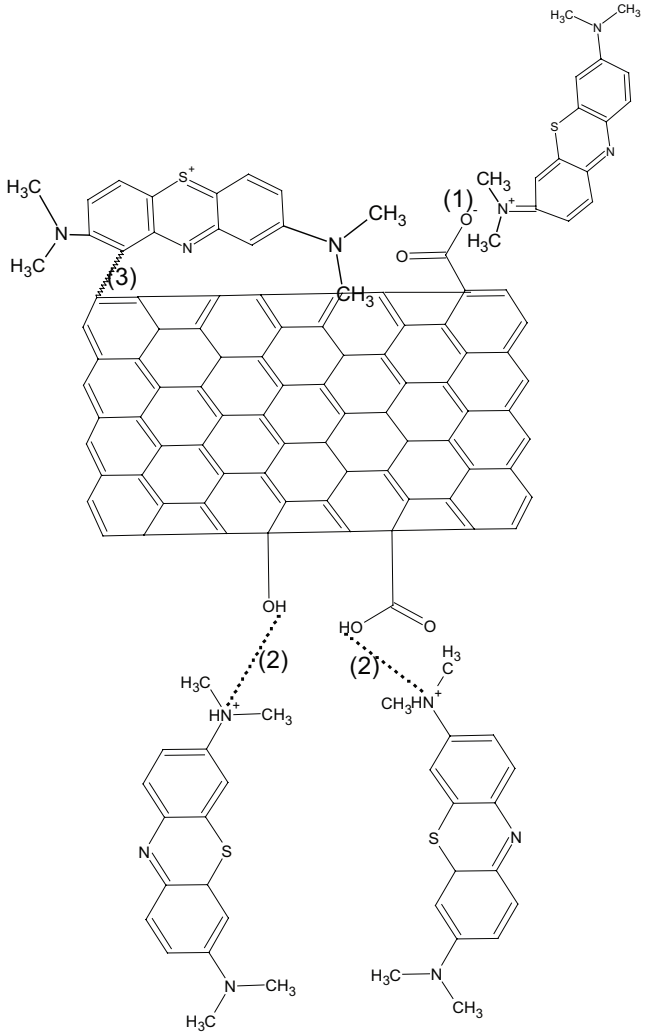

Fig. 15. MB–mCNTs interaction: (1) ionic interaction (involves pH of experimental solution), (2) hydrogen bonding (the connection between hydroxyl and carboxyl groups on mCNTs and the positive electric element nitrogen in MB molecule), (3) π-π stacking (stacking of benzene ring on MB and mCNTs).

Under acidic conditions, –COOH or –OH on the adsorbent surface can form hydrogen bonds with the positive nitrogen charge on MB. With the increase of pH, –COOH became –COO$^-$ and the electrostatic attraction between –COO$^-$ and MB with positive charge increased, resulting in the increase of the adsorption capacity. In addition, mCNTs and MB had both a large number of benzene rings, which can be line into a π-π conjugate. Fig. 15 shows the interaction between mCNTs and MB.

4. Conclusion

In this paper, the mCNTs was prepared by modified multi-walled carbon nanotubes with a simple and readily available sodium hypochlorite solution. The effects of adsorbent dosage, salt, temperature and time were studied. The results showed that salt coexisted in solution was dis-

advantage of adsorption and it was fast to reach adsorption equilibrium. The pseudo-first order kinetic model and the pseudo-second order model were both well to fit kinetic process while Koble-Corrigan model was best to predict the equilibrium process. The thermodynamic parameters indicated that the process was spontaneous and exothermic. Furthermore, there was high adsorption quantity of CR on MB-loaded mCNTs in second adsorption. It was implied that mCNTs be promising as adsorbent to remove dyes from solution.

References

[1] P. Kumar, B. Prasad, I.M. Mishra, S. Chand, Decolorization and COD reduction of dyeing wastewater from a cotton textile mill using thermolysis and coagulation, J. Hazard. Mater., 153 (2008) 635–645.

[2] A.K. Verma, R.R. Dash, P. Bhunia, A review on chemical coagulation/flocculation technologies for removal of colour from textile wastewaters, J. Environ. Manage., 93 (2012) 154–168.

[3] M.F. Abid, M.A. Zablouk, A.M. Abid-Alameer, Experimental study of dye removal from industrial wastewater by membrane technologies of reverse osmosis and nanofiltration, Iran. J Environ. Health., 9 (2012) 17–23.

[4] S. Rengaraj, K.H. Yeon, S.H. Moon, Removal of chromium from water and wastewater by ion exchange resins, J. Hazard. Mater., 87 (2015) 273–287.

[5] D. Lee, J.C. Lee, J.Y. Nam, H.W. Kim, Degradation of sulfonamide antibiotics and their intermediates toxicity in an aeration-assisted non-thermal plasma while treating strong wastewater, Chemosphere, 209 (2018) 901–907.

[6] X. Xu, B.Y. Gao, B. Jin, Q.Y. Yue, Removal of anionic pollutants from liquids by biomass materials: A review, J. Mol. Liq., 215 (2016) 565–595.

[7] B.L. Zhao, W. Xiao, Y. Shang, H.M. Zhu, R.P. Han, Adsorption of light green anionic dye using cationic surfactant-modified peanut husk in batch mode, Arab. J. Chem., 10 (2017) s3595–s3602.

[8] M.T. Yagub, T.K. Sen, S. Afroze, H.M. Ang, Dye and its removal from aqueous solution by adsorption: A review, Adv. Colloid Interface, 209 (2014) 172–184.

[9] S. Iijima, Helical microtubules of graphitic carbon, Nature, 354 (1991) 56–58.

[10] X. Wang, Q. Li, X. Jing, J. Zhong, J. Wang, L. Yan, K. Jiang, S. Fan, Fabrication of ultralong and electrically uniform single-walled carbon nanotubes on clean substrates, Nano Lett., 9 (2009) 31–37.

[11] T.A. Saleh, The influence of treatment temperature on the acidity of MWCNT oxidized by HNO_3 or a mixture of HNO_3/H_2SO_4, Appl. Surf. Sci., 257 (2011) 7746–7751.

[12] D.D. Chronopoulos, C.G. Kokotos, N. Karousis, G. Kokotos, N. Tagmatarchis, Functionalized multi-walled carbon nanotubes in an aldol reaction, Nanoscale, 7 (2015) 2750–2757.

[13] O. Dutko, D. Plachá, M. Mikeska, G.S. Martynková, P. Wróbel, A. Bachmatiuk, M.H. Rümmeli, Comparison of selected oxidative methods for carbon nanotubes: structure and functionalization study, J. Nanosci. Nanotechnol., 16 (2016) 7822–7825.

[14] C.H. Wu, Adsorption of reactive dye onto carbon nanotubes: equilibrium, kinetics and thermodynamics, J. Hazard. Mater., 144 (2007) 93–100.

[15] C. Lu, C. Liu, F. Su, Sorption kinetics, thermodynamics and competition of Ni^{2+} from aqueous solutions onto surface oxidized carbon nanotubes, Desalination, 249 (2009) 18–23.

[16] Y.J. Zhang, J. Yang, B.L. Liu, Y.D. Xu, Removal of copper ions from water using chemical modified multi-walled carbon nanotubes, J. Chem. Soc. Pak., 36 (2014) 841–847.

[17] F. Yu, J. Ma, Y. Wu, Adsorption of toluene, ethylbenzene and xylene isomers on multi-walled carbon nanotubes oxidized by different concentration of NaOCl, Front. Env. Sci. Eng., 6 (2011) 320–329.

[18] Q.Q. Zhao, J.Q. Bi, W.L. Wang, G.X. Sun, A novel method of functionalizing carbon nanotubes via neutralization reaction, Mater. Lett., 185 (2016) 523–525.

[19] F. Su, C. Lu, S. Hu, Adsorption of benzene, toluene, ethylbenzene and p-xylene by NaOCl-oxidized carbon nanotubes, Colloid. Surfaces A, 353 (2010) 83–91.

[20] P. Nie, C.Y. Min, H.J. Song, X.H. Chen, Z.Z. Zhang, K.L. Zhao, Preparation and tribological properties of polyimide/carboxyl-functionalized multi-walled carbon nanotube nanocomposite films under seawater lubrication, Tribol. Lett., 58 (2015) no 7.

[21] R.P. Han, P. Han, Z.H. Cai, Z.H. Zhao, M.S. Tang, Kinetics and isotherms of neutral red adsorption on peanut husk, J. Environ. Sci.-China, 20 (2008) 1035–1041.

[22] R.P. Han, W.H. Zou, J.H. Zhang, J. Shi, Characterization of chaff and biosorption of copper and lead ions from aqueous solution, Acta Sci. Circumst., 26 (2006) 32–39.

[23] Y.C. Rong, H. Li, L.H. Xiao, Q. Wang, Y.Y. Hu, S.S. Zhang, R.P. Han, Adsorption of malachite green dye from solution by magnetic activated carbon in batch mode, Desal. Water Treat., 106 (2018) 273–284.

[24] Y.F. Gu, M.Y. Liu, M.M. Yang, W.L. Wang, S.S. Zhang, R.P. Han, Adsorption of light green anionic dye from solution using polyethyleneimine modified carbon nanotubes in batch mode, Desal. Water Treat., 138 (2019) 368–378.

[25] Y. Yao, F. Xu, M. Chen, Z. Xu, Z. Zhu, Adsorption behavior of methylene blue on carbon nanotubes, Bioresour. Technol., 101 (2010) 3040–3046.

[26] J.Y. Song, W.H. Zou, Y.Y. Bian, F.Y. Su, R.P. Han, Adsorption characteristics of methylene blue by peanut husk in batch and column mode, Desalination, 265 (2011) 119–125.

[27] Y.S. Ho, J.C.Y. Ng, G. McKay, Kinetics of pollutant sorption by biosorbents: review, Sep. Purif. Method., 29 (2000) 189–232.

[28] J. Ma, L.L. Yu, L. Jin, Z.W. Yuan, J.H. Chen, Study on adsorption properties of methylene blue on original carbon nanotubes, Environ. Chem., 31 (2012) 646–652 (in Chinese).

[29] Z. Aksu, Application of biosorption for the removal of organic pollutants: a review, Process Biochem., 40 (2005) 997–1026.

[30] Y. Shang, J.H. Zhang, X. Wang, R.D. Zhang, W. Xiao, S.S. Zhang, R.P. Han, Use of polyethylenemine modified wheat straw for adsorption of congo red from solution in batch mode, Desal. Water Treat., 57 (2016) 8872–8883.

[31] M.Y. Han, Q. Wang, H. Li, L.Y. Fang, R.P. Han, Removal of methyl orange from aqueous solutions by polydopamine mediated surface functionalization of Fe_3O_4 in batch mode, Desal. Water Treat., 115 (2018) 271–280.

[32] Z. Aksu, Determination of the equilibrium, kinetic and thermodynamic parameters of the batch biosorption of nickel(II) ions onto Chlorella vulgaris, Process Biochem., 38 (2002) 89–99.

[33] B.H. Hameed, Equilibrium and kinetics studies of 2,4,6-trichlorophenol adsorption onto activated clay, Colloid. Surface. A, 307 (2007) 45–52.

[34] R.P. Han, Y. Wang, Q. Sun, L.L. Wang, J.Y. Song, X.T. He, C.C. Dou, Malachite green adsorption onto natural zeolite and reuse by microwave irradiation, J. Hazard. Mater., 175 (2010) 1056–1061.

[35] H.N. Bhatti, A. Jabeen, M. Iqbal, S. Noreen, Z. Naseem, Adsorptive behavior of rice bran-based composites for malachite green dye: Isotherm, kinetic and thermodynamic studies, J. Mol. Liq., 237 (2017) 322–333.

[36] Y.B. Jiao, D.L. Han, Y.Z. Lu, Y.C. Rong, L.Y. Fang, Y.L. Liu, R.P. Han, Characterization of pine-sawdust pyrolytic char activated by phosphoric acid through microwave irradiation and adsorption property toward CDNB in batch mode, Desal. Water Treat., 77 (2017) 247–255.

[37] M.Y. Liu, X.Y. Li, Y.Y. Du, R.P. Han, Adsorption of methyl blue from solution using walnut shell and reuse in a secondary adsorption for congo red, Bioresour. Technol. Rep., 5 (2019) 238–242.

[38] J.F. Miao, L.F. Liu, Y.Z. Lu, Y.Q. Song, R.P. Han, Reuse of neutral red-loaded wheat straw for adsorption of congo red from solution in a fixed-bed column, Adv. Eng. Res., 76 (2016) 332–336.

[39] R.D. Zhang, J.H. Zhang, X.N. Zhang, C.C. Dou, R.P. Han, Adsorption of Congo red from aqueous solutions using cationic surfactant modified wheat straw in batch mode: Kinetic and equilibrium study, J. Taiwan Inst. Chem. E., 45 (2014) 2578–2583.
[40] Y.Y. Su, B.L. Zhao, W. Xiao, R.P. Han, Adsorption behavior of light green anionic dye using cationic surfactant-modified wheat straw in batch and column mode, Environ. Sci. Pollut. R., 20 (2013) 5558–5568.
[41] H. Yan, W.X. Zhang, X.W. Kan, L. Dong, Z.W. Jiang, H.J. Li, H. Yang, R.S. Cheng, Sorption of methylene blue by carboxymethyl cellulose and reuse process in a secondary sorption, Colloid. Surface. A, 380 (2011) 143–151.
[42] M.Y. Liu, J.J. Dong, W.L. Wang, M.M. Yang, Y.F. Gu, R.P. Han, Study of methylene blue adsorption from solution by magnetic graphene oxide composites, Desal. Water Treat., 147 (2019) 398–408.